https://doi.org/10.15407/ufm.23.04.613

I.M. PAZUKHA* and Yu.O. SHKURDODA**
Sumy State University,
2 Rimsky-Korsakov Str., UA-40007 Sumy, Ukraine
* i.pazukha@aph.sumdu.edu.ua, ** yu.shkurdoda@gmail.com

CRYSTAL STRUCTURE, PHASE STATE, AND MAGNETORESISTIVE PROPERTIES OF NANOSTRUCTURED THIN-FILM SYSTEMS BASED ON PERMALLOY AND NOBLE METALS

We review and analyse the literature data on the experimental results dealing with the crystal structure, phase state, and magnetoresistive properties of nanostructured thin-film systems based on Ni_xFe_{1-x} permalloy and noble metals prepared by the methods of co-evaporation and layer-by-layer condensation. As shown, regardless of preparation methods, the phase state of systems stays as two-phase one. Upon high-temperature annealing, the formation of solid solutions is possible. As shown, in the case of applying of layer-by-layer condensation method, the value of the magnetoresistive effect depends on the thickness of the magnetic and nonmagnetic layers. In the case of applying the co-evaporation method, the determining parameters are the concentrations of the components and the total thickness of the system. The annealing-temperature effect on magnetoresistive properties of nanostructured thin-film systems based on permalloy and noble metals is analysed.

Keywords: permalloy, noble metal, crystal structure, phase state, magnetoresistance, concentration effect, temperature effect.

1. Introduction

Among ferromagnetic materials used in the field of data storage technology or as a magnetoresistive sensor, permalloy can be distinguished [1, 2]. Permalloy is a soft ferromagnetic alloy based on Ni and Fe (Ni_xFe_{1-x}), containing up to 50 at.% of Fe. It is characterized by low-value coercivity, high saturation magnetization, and high susceptibility [3–7]. To extend

Citation: I.M. Pazukha and Yu.O. Shkurdoda, Crystal Structure, Phase State, and Magnetoresistive Properties of Nanostructured Thin-Film Systems Based on Permalloy and Noble Metals, *Progress in Physics of Metals*, **23**, No. 4: 613–628 (2022)

the fields of permalloy practical application, it combines with nonmagnetic metal (NM). For the formation of nanostructured thin-film systems based on Ni_xFe_{1-x} and NM, the methods of layer-by-layer deposition and co-evaporation are used. Using the methods of layer-by-layer condensation, multilayer structures of both general and periodic types can be formed. At the same time, the co-evaporation method allows for the formation of granular alloy and composite materials.

Trilayer systems like $FM_1/NM/FM_2$ [8, 9], multilayers $[FM/NM]_n$ [10–13], and spin-valve structures (classical $AFM/FM_1/NM/FM_2$ and modifications) [14–17] should be attributed to the general type; as usual, FM denotes ferromagnetic metal Co, Ni, Fe or their alloys. NM is nonmagnetic transition metal (V, Cr, Nb, Mo, Ru, *etc.*) or noble metal (Cu, Ag, and Au). AFM denotes antiferromagnetic material, like FeMn. Among permalloys, $Ni_{80}Fe_{20}$ and $Ni_{50}Fe_{50}$ alloys found the most practical application. Note that, in the first spin-valve structure, which was fabricated by B. Denny [14] in 1991, permalloy $Ni_{80}Fe_{20}$ was used as a material of free and fixed layers. Later on, various ways of modifying the $Ni_{80}Fe_{20}/Cu/Ni_{80}Fe_{20}/Fe_{50}Mn_{50}$ spin-valve, proposed by B. Denny, were developed. Including ferromagnetic Ni_xFe_{1-x} alloys are used as one of the functional layers of spin-valves [13, 17, 18].

Fairly often, the attention of researchers is attracted by two-layer structures like Ni_xFe_{1-x}/NM [19, 20] or Ni_xFe_{1-x}/AFM [21, 22]. For example, in Ref. [20], denoted two-layer system $Ni_{80}Fe_{20}$/Ag was demonstrated following. It is a result of thermomagnetic cooling–heating within the temperature range of 5–300 K. Therefore, it can change the magnetoresistive properties of the neighbouring ferromagnetic layer. It is especially true, when the spin-diffusion length has the same order of magnitude as the sample thickness. The effect of exchange interaction that arises at the ferromagnetic–antiferromagnetic interfaces was investigated in Ref. [23].

In the formation of granular alloys or composite material by the co-evaporation methods, as a rule, two components (magnetic and nonmagnetic ones) with low mutual solubility are used. It allows realizing the nanostructures, which consist of magnetic nanoparticles embedded into the nonmagnetic matrix. Co, Ni, Fe, and their alloys are often used as ferromagnetic components. Noble metals (Cu, Ag, Au, and Pt) [24–27] or insulators (SiO_x, Al_2O_3) [28–31] are used as nonmagnetic matrix.

This work focuses on reviewing and analysing the literature data concerned with the study of ferromagnetic nanostructures based on Ni_xFe_{1-x} alloys and noble metals prepared by the methods of co-evaporation and layer-by-layer condensation. Namely, we analyse their crystal structure, phase state, and magnetoresistive properties after condensation and in the condition of heat treatment within the wide temperature range.

2. Crystal Structure and Phase State

The method of formation of nanodimensional structures (co-evaporation or layer-by-layer ones) can significantly affect diffusion processes at the condensation state and upon annealing. At this, the phase state of a system can change and lead to solid solution formation. From the point of analysis of magnetoresistive properties, exactly, the phase state of the magnetic component is important. The nature of the crystalline structure of the studied materials is no less important. The change of mean grain size of magnetic components can change their magnetic state from superparamagnetic-to-ferromagnetic one [32]. Especially, it is essential for structures, which are prepared by the co-evaporation method. Depending on the mean size, magnetic granules formed in the bulk of nonmagnetic matrix can be superparamagnetic, single- or multidomain ferromagnetic [33]. These states exhibit different magnetic properties and affect the nature and amplitude of magnetoresistive effects.

Detail analysis of phase state of the as-deposited trilayer Fe_xNi_{100-x}/Cu/Fe_xNi_{100-x} samples with the thicknesses of magnetic layers d_F = 10–50 nm and nonmagnetic one d_N = 5–50 nm at $c_{Ni} \cong$ 50–80 at.% was done in Ref. [34]. It was demonstrated that the phase state of the system corresponds to the combination of the two face-centred cubic lattices f.c.c.-Ni_3Fe and f.c.c.-Cu (Fig. 1, *a*, *b*). The annealing of the trilayer Fe_xNi_{100-x}/Cu/Fe_xNi_{100-x} system at the temperature of 700 K leads to solid solution formation. At $c_{Ni} \cong$ 80 at.%, the Ni_3Fe(Cu) solid solution is formed (Fig. 1, *b*). At the same time, decrease of c_{Ni} to 50 at.% leads to the NiFe(Cu) solid solution formation (Fig. 1, *d*).

The concentration effect in phase state and crystal structure of ($Ni_{50}Fe_{50}$+Cu)/*S* system was analysed in Ref. [35]. The samples were prepared by simultaneous magnetron sputtering at room temperature. The concentration of Cu atoms changes within the range from 58 to 85%. It was demonstrated that (111), (200), (220), and (311) lines are fixed at the diffraction patterns regardless of the composition of samples. At this, the (110) line that belongs to the b.c.c.-NiFe lattice coincides with the (111) line of f.c.c.-Cu. No other line corresponding to b.c.c.-NiFe is fixed. According to Ref. [35], this indicates the fact that due to the small size of the nanoparticles of the magnetic component, they form an amorphous structure. Note, Ni_xFe_{100-x} alloys are characterized by the formation of an amorphous structure at the early condensation stages, which subsequently crystallizes. Increasing the volume fraction of $Ni_{50}Fe_{50}$ nanoparticles leads to their mean grain size growth. It is accompanied by isolating the b.c.c. phase from the Cu matrix and the increase in the intensity of the (200) line of b.c.c.-NiFe.

The analysis of crystal structures confirms [35] that as-deposited ($Ni_{50}Fe_{50}$ + Cu)/*S* thin films consist of $Ni_{50}Fe_{50}$ nanoparticles uniformly

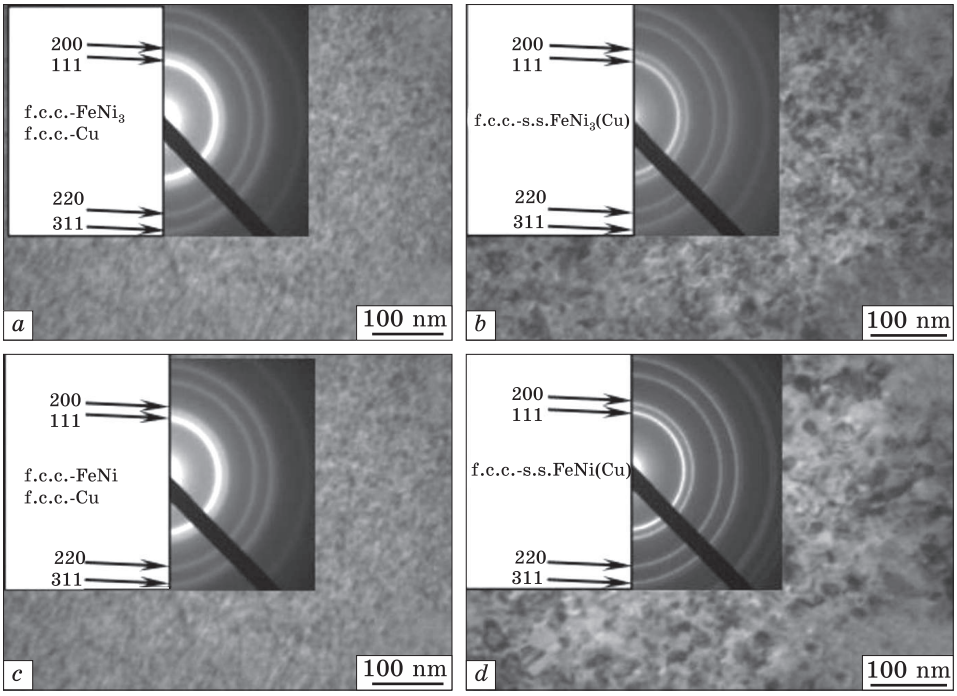

Fig. 1. Bright-field transmission electron microscopy (TEM) images and diffraction patterns of $Fe_xNi_{100-x}(35)/Cu(10)/Fe_xNi_{100-x}(35)/S$ three-layer film systems at x = 20 at.% (*a*, *b*) and x = 60 at.% (*c*, *d*) after deposition (*a*, *c*) and annealing at a temperature of 700 K (*b*, *d*) [34]

distributed in the Cu matrix (Fig. 2). At the low fraction of the magnetic component, $Ni_{50}Fe_{50}$ nanoparticles surrounded by the Cu matrix have an equilibrium form. At the increase in volume fraction of magnetic component, $Ni_{50}Fe_{50}$ nanoparticles gradually deviate from the equilibrium form. Calculations showed that the increase in volume fraction of magnetic components from 15 to 42% leads to the growth of the mean size of magnetic nanoparticles from 2 to 6 nm.

The same results were obtained in Ref. [37] for $(Fe_{80}Ni_{20} + Cu)/S$ thin-film system at c_{Cu} = 60 at.% that has a two-face state after condensation. The mean size of nanoparticles of a magnetic component, according to Ref. [37], is of 5 nm. During the annealing at a temperature of 673 K for 60 min, the insignificant growth of magnetic nanoparticles size to 7 nm occurs. The increase of the annealing time to 240 min. leads to the coalescence of magnetic grains and increases their mean size to 13 nm.

The research on the phases state of $[Ni_{81}Fe_{19}(2)/Ag(4)]_{20}/S$ multilayers by the method of x-ray diffraction [37] showed that a strong texture (111) is formed during condensation. This indicates the high quality of the multilayers. Calculations of the interplanar distances d_{111} for the

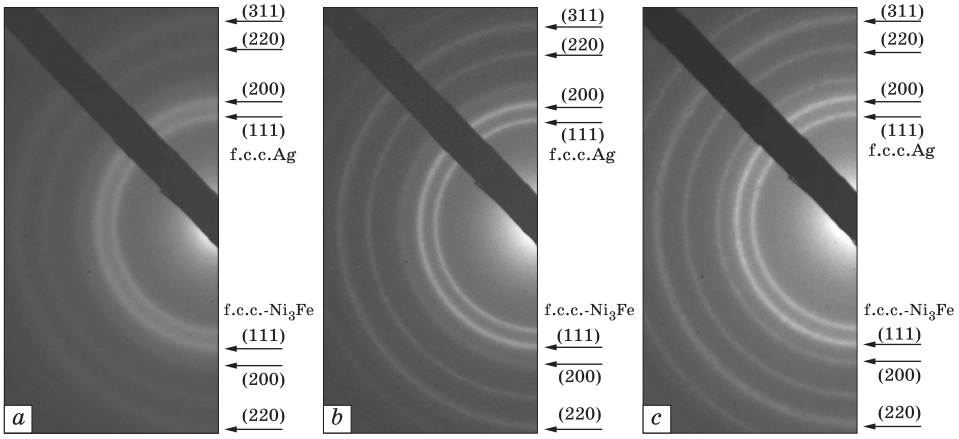

Fig. 2. Diffraction patterns of the $(Ni_{80}Fe_{20} + Ag)/S$ film systems with d = 55 nm and c_{Ag} = 60 at.% after deposition (*a*) and heat treatment at 500 (*b*) and 700 K (*c*) [39]

f.c.c.-Ni_3Fe and f.c.c.-Ag phases indicate a slight deviation from the tabular data. For the f.c.c.-Ni_3Fe phase, the value of d_{111} = 0.2048 nm is slightly smaller than the tabular data (d_{111} = 0.205 nm). For the f.c.c.-Ag phase, the value of d_{111} = 0.2354 nm is slightly increased compared with the tabular data (d_{111} = 0.235 nm). The low value of the roughness of interfaces h = 0.16 nm indicates the perfection of both magnetic and nonmagnetic layers throughout the thickness of the multilayer. According to Ref. [37], the fact that both materials have parameters of interplanar distances close to the data for bulk materials indicates the following. Layers grow incoherently. The dislocations, rather than the expansion and contraction of a single lattice, cause deformation at the interface. The same conclusion was done in Ref. [38].

Results of the investigation of phase state, crystal structure, and magnetoresistive properties of $(Ni_{80}Fe_{20} + Ag)/S$ thin films with d = 55 nm and c_{Ag} = 10–85 at% in as-deposited and annealed states were presented in Ref [39]. Electron-diffraction patterns for as-deposited and annealed at 500 and 700 K $(Ni_{80}Fe_{20} + Ag)/S$ thin films at c_{Ag} = 60 at.% shown that samples before and after annealing have a two-phase state f.c.c.-Ni_3Fe + f.c.c.-Ag (Fig. 2). Analysis of a series of bright-field TEM images (positions *1*–*4* in Fig. 3) demonstrates that the transition in the crystal structure of samples with increasing c_{Ag} is occurring. Position *1* in Fig. 3 illustrates the structure consisted of nonmagnetic grains embedded into the ferromagnetic matrix. At the same time, position *4* in Fig. 3 shows the structure where ferromagnetic grains are embedded into the nonmagnetic matrix. This transition is accompanied by the increase in the grain mean size, which slightly changes during annealing at 500 K (Fig. 3, *b*). The effect of annealing at 700 K on the crystal structure of

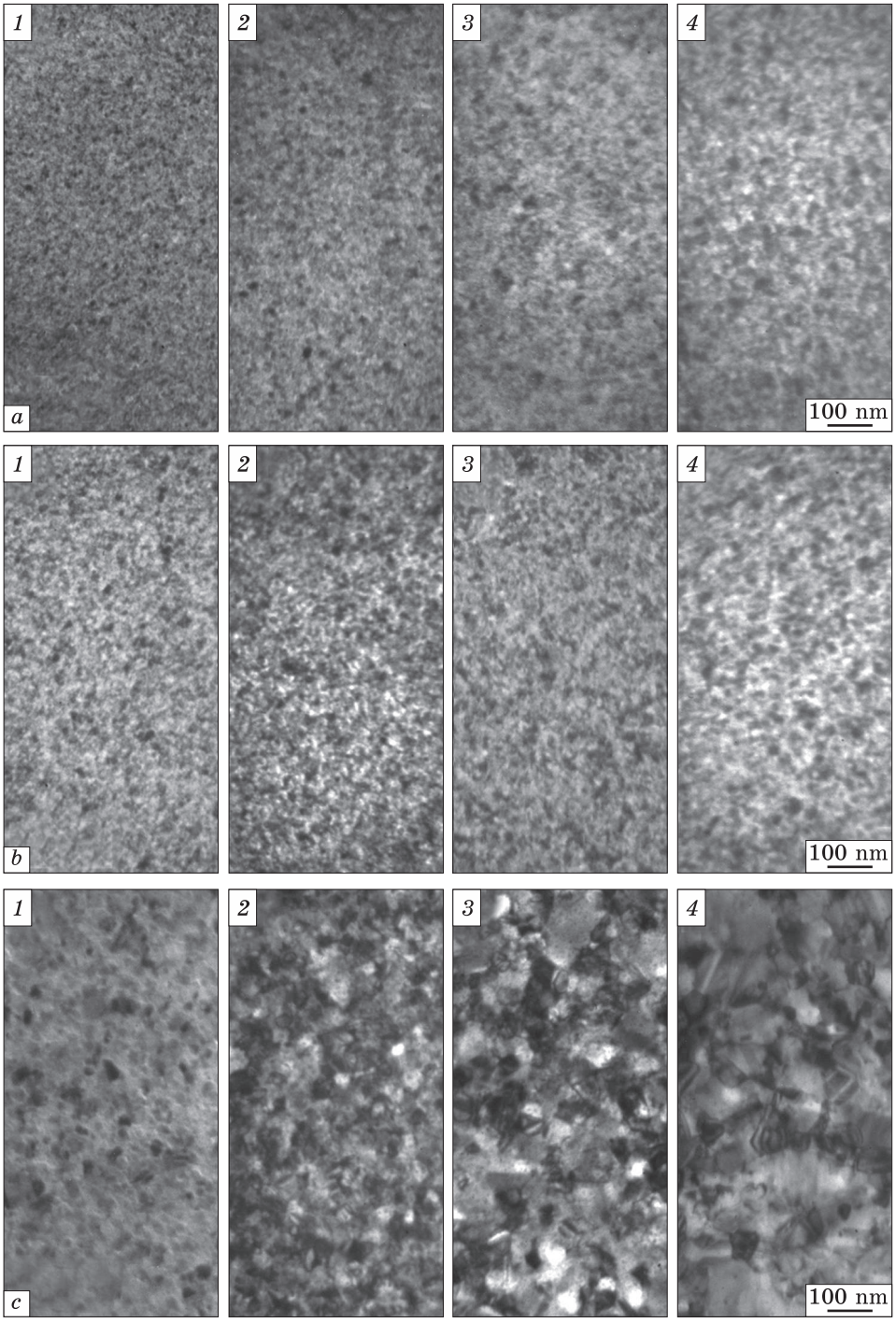

Fig. 3. Bright-field TEM images of the $(Ni_{80}Fe_{20} + Ag)/S$ film systems with $d = 55$ nm and $c_{Ag} = 20$ (*1*), 32 (*2*), 60 (*3*), and 78 at.% (*4*) after deposition (*a*) and heat treatment at 500 (*b*) and 700 K (*c*) [39]

thin films is different depending on c_{Ag} (Fig. 3, *c*). For the film with a low-concentration nonmagnetic material, the Ag grain growth stagnation occurs because of their isolation in the ferromagnetic matrix. At the Ag concentration in the range of 32–60 at.%, the grains of two types can be identified at the TEM-images: nanosize (2–5 nm) grains and grains with the average size of about 50 nm, which correspond to $Ni_{80}Fe_{20}$ and Ag, respectively (Fig. 3, *c*, positions *2* and *3*). In the case of high Ag concentration, the crystal structure of the films can be described as small ferromagnetic grains, which are randomly distributed within the volume of nonmagnetic material.

Thus, the analysis of the data denoted crystal structure and phase state of nanostructured thin-film systems based on permalloy and noble metals, the following should be noted. For as-deposited systems based on Ni_xFe_{1-x} and Cu, Ag, or Au, regardless of preparation method (layer-by-layer of co-evaporation), the two-phase state retains. The formation of solid solutions is possible under heat treatment. The structure of the samples both before and after heat treatment at a temperature of 750 K remains nanodimensional. The average size of magnetic grains does not exceed 10 nm in the as-deposited state. Only the high-temperature annealing at 900 K causes their growth to 20 nm.

3. Peculiarity of Magnetoresistive Properties

3.1. Nanostructured Thin-Film Systems Prepared by the Layer-by-Layer Condensation Method: $Ni_xFe_{1-x}/NM/Ni_xFe_{1-x}$ and $[Ni_xFe_{1-x}]_n$

During the last decades, the different nanostructured thin-film systems prepared by the layer-by-layer condensation method are widely investigated. Namely, these are three-layer $Ni_xFe_{1-x}/NM/Ni_xFe_{1-x}$ and multilayer $[Ni_xFe_{1-x}]_n$ systems. Various scientific groups are still trying to improve such structures with the purpose to expand the areas of their practical application.

The results of research on magnetoresistive properties for $[NiFe/Cu]_n$ multilayers are presented in Refs. [11, 40]. It was demonstrated that the value *MR* of the magnetoresistive (MR) effect strongly depends on the thickness of magnetic and nonmagnetic layers. The maximum value of 10% was obtained at d_{NiFe} = 3 nm and d_{Cu} = 1 nm. In more cases devoted to the giant magnetoresistance (GMR) investigations in $[Ni_xFe_{1-x}/Ag]_n$, a large enough value of the effect magnitude does not obtained. For example, for $[Ni_{81}Fe_{19}(2)/Ag(4)]_{20}/S$ multilayer, the value of magnetoresistance does not exceed 0.2% [36]. During the annealing process at a temperature of 673 K, the increase of *MR* value by 4.5 times occurs. This is associated with the diffusion of Ag atoms through the magnetic layers, which causes the isolation of crystallites of the magnetic component in

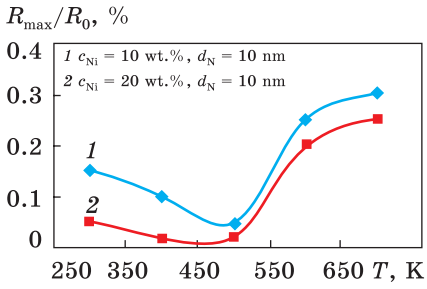

Fig. 4. Isotropic magnetoresistance as a function of the annealing temperature for the $Fe_xNi_{100-x}/Cu/Fe_xNi_{100-x}$ systems at $d(Fe_xNi_{100-x})$ = 10 nm and two Ni concentrations (c_{Ni}) in the magnetic layers [43]

the nonmagnetic matrix and the formation of a granular structure. In this case, the GMR effect is realized as a result of spin-dependent electron scattering at the interfaces 'magnetic grain/nonmagnetic matrix' and in the volume of magnetic grains. However, the increase in annealing time leads to a fall in *MR* magnitude. A result of the magne-tic grain growth and coalescence causes the transition of magnetic grains in the multidomain state and reduces the efficiency of spin-dependent scattering.

Exceptions are data presented in Refs. [41, 42]. For $[Ni_{81}Fe_{19}(1.2)/Ag(d_{Ag})]_n/S$ and $[Ni_{81}Fe_{19}(2.6)/Ag(d_{Ag})]_n/S$ with a total thickness of 500 nm, the maximum value of the GMR effect (11%) can be achieved at a thickness of the nonmagnetic layer of 1.1 nm. At this thickness, the antiferromagnetic connection between the magnetic layers is realized. Upon thermomagnetic annealing at a temperature of 523 K and under a magnetic field of 0.4 T, the *MR* value increases up to 12.2%. According to Ref. [41], this is a result of magnetic field application, rather than structural changes in the sample.

Among three-layer $Ni_xFe_{1-x}/NM/Ni_xFe_{1-x}$ systems, the system $Ni_xFe_{1-x}/Cu/Ni_xFe_{1-x}$ is the most studied. Detail analysis of the nature of the field dependences for samples in the as-deposited state and after annealing within the temperature range from 300 to 700 K was carried out in Refs. [33, 43]. These investigations were done taking into account the effect of Ni content in the ferromagnetic alloy Ni_xFe_{1-x} as well as the thickness of the nonmagnetic layer on the amplitude of the magnetoresistive effect.

In particular, it was demonstrated that the thin-film granular alloy can be obtained by the method of layer-by-layer condensation under conditions of ultrathin magnetic layers (d = 0.5–0.8 nm) or thicker ones (d = 1–10 nm) followed by vacuum heat treatment in the temperature range 500–700 K.

The results of investigation of magnetoresistive properties of thin-film granular alloys prepared by the method of layer-by-layer condensation of Fe_xNi_{1-x} (x = 0.7–0.9; $d(Fe_xNi_{1-x}$ = 5–10 nm) and d(Cu) = 10–20 nm at room temperature with subsequent heat treatment presented in Ref. [43]. Note that such samples have a phase state b.c.c.-Fe-Ni + f.c.c.-Cu.

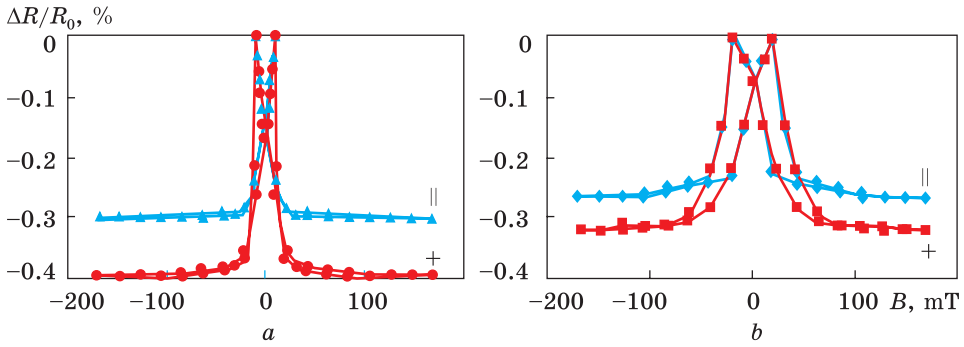

Fig. 5. Field dependences of longitudinal (||) and transverse (+) magnetoresistance for the as-deposited (*a*) and annealed at 700 K (*b*) trilayer $Fe_xNi_{100-x}/Cu/Fe_xNi_{100-x}$ thin films with $d(Fe_xNi_{100-x})$ = 10 nm, d(Cu) = 10 nm, c_{Ni} = 20 wt.%. The measurement temperature is of 300 K [43]

The layer-by-layer analysis by secondary ion mass spectrometry showed complete diffusion mixing of the components. It allows concluding that the transition from the layered structure in the as-deposited state to granular one in the annealed state occurs. The temperature dependence of magnetoresistance, which is presented in Fig. 4, confirms this too. As can be seen from Fig. 4, for samples in the as-deposited state, the isotropic magnetoresistance of 0.1–0.2% is fixed. It evidences the realization of spin-dependent electron scattering in a three-layer structure. The annealing at a temperature of 500 K leads to a significant decrease of isotropic magnetoresistance up to 0.02–0.05%. The reason is by disruption of the structural integrity of the Cu interlayer. The increase of annealing temperature to 600 K causes the rise of *MR* value as a result of granular state formation.

To establish the causes of isotropic magnetoresistance changes, the analysis of the change of resistivity ρ and the value of ΔR_{max} for the first cycle of heating was done [43]. It was noted that, for all samples, the value of resistivity is irreversibly decreased from $(40–55)\cdot10^{-7}$ Ohm·m to $(10–20)\cdot10^{-7}$ Ohm·m upon annealing at 500 K. The rise of annealing temperature to 600 and 700 K does not lead to significant changes in resistivity. The large values of resistivity of trilayer systems (in comparison with values of resistivity for the pure metal in the bulk state) can be explained by more defect structures of thinnest layers and occurrence of defects at the interfaces of layers, on the one hand, and by the small size of crystallites (compared to the bulk state) and size effects in electrical conductivity, on the other hand. Simultaneously, the value of ΔR_{max} decreases by 5–10 times after annealing to 500 K. This indicates that a significant number of microholes have appeared in the Cu layer. As a result, the direct connection between the magnetic layers is realized that prevents their separate remagnetization. This

significantly reduces the role of spin-dependent electron scattering. After annealing to 600 K, the value of ΔR_{max} increases by 5–7 times. This is a result of a significant increase in the probability of spin-dependent electron scattering due to the granular state. The changes of ρ and ΔR_{max} values cause a nonmonotonic change in the magnetoresistive ratio $\Delta R_{max}/R_0$.

Figure 5 illustrates the results of investigations of $MR(B)$ dependences for the $Fe_{0.8}Ni_{0.2}$(10 nm)/Cu(20 nm)/$Fe_{0.8}Ni_{0.2}$(10 nm)/S three-layer system after deposition and annealing to 700 K [43]. In this case, the negative isotropic magnetoresistive effect is observed. Namely, the resistance is decreased in the external magnetic field independently on the mutual orientation of field, current, and sample. Therefore, this allows concluding that GMR is realized in the granular alloys prepared by the method of layer-by-layer condensation with subsequent annealing. The reasons for GMR appearing can be explained within the scope of realization of spin-dependent electron scattering at the surfaces and in the volume of the granules. Note, the insignificant discrepancy of field dependences measured in longitudinal and transverse geometries in the fields more than in saturation field due to the influence of anisotropic magnetoresistance of ferromagnetic granules and clusters.

3.2. Nanostructured Thin-Film Systems Prepared Using the Co-Evaporation Method (Ni_xFe_{1-x} + NM)

When nanostructured thin films are prepared by the co-evaporation method, the granular structure is formed. Nanosize magnetic particles separate in the volume of the nonmagnetic matrix. The size of magnetic particles depends on the degree of solubility of the two materials and the temperature of the substrate (S) during deposition. As a result, the magnetoresistive properties of such systems can be quite different due to significant changes in the size of magnetic nanoparticles and the width of nonmagnetic channels. According to Ref. [44], there are three main contributions to their magnetoresistance. The first one is a giant magnetoresistance, the nature of which is the same as in multilayers. The second one is a scattering at the magnetic fluctuations. This component of the magnetoresistance exists in any ferromagnetic material around the ordering temperature. The third one is anisotropic magnetoresistance associated with spin–orbit interaction in a magnetic material.

For the first component to be dominant, certain conditions must be met. First, the concentration of magnetic components does not of a certain value to prevent the formation of multidomain ferromagnetic nanoparticles. Second, paramagnetic oscillations, which occur above the ordering temperature in the shell of magnetic particles, should be minimized because they induce a strong ‘spin-flip’ dispersion of conduction

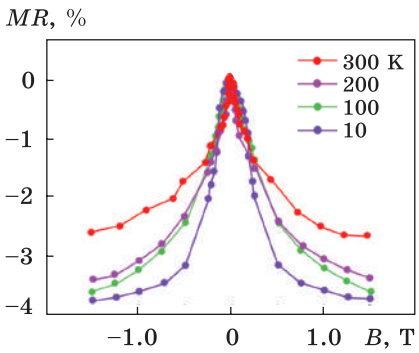

Fig. 6. Field dependences of magnetoresistance measured at different temperatures for the as-deposited $(Ni_{80}Fe_{20} + Ag)/S$ system with d = 60 nm and c_{Ag} = 60 at.% [49]

electrons. Third, the distance between the magnetic particles must be less than the diffusion length of the spin-flip in the nonmagnetic matrix. This distance should be as small as possible (to avoid parasitic scattering in the nonmagnetic matrix) but does not cause ferromagnetic interactions between magnetic grains. The optimal particle size is not easy to predict. It depends on several parameters. It depends on the mean free path of the charge carriers in magnetic and nonmagnetic materials. Besides, the relative contribution of spin-dependent scattering in the volume of magnetic particle and at the interfaces 'magnetic particle–nonmagnetic matrix' has significant influence too.

An analysis of the literature [35, 36, 44–46] devoted to the study of magnetoresistive properties of $(Ni_xFe_{1-x} + NM)/S$ thin films prepared by the co-evaporation technique confirms the conclusion that the value and nature of magnetoresistive effect strongly depends on composition of the samples. Theoretical and experimental studies of the GMR effect [47, 48] evidence that the presence of multidomain magnetic nanoparticles negatively affects the efficiency of spin-dependent scattering. At the same time, the presence of superparamagnetic and single-domain magnetic nanoparticles plays a key role. Authors of Refs. [47, 48] demonstrated that a certain monotonic dependence between the size of nanoparticles and the value of the effect is absent. For each system with GMR, the maximum value of the effect is fixed at a certain average size of magnetic nanoparticles at a given temperature of heat treatment.

For instance, the value of MR for system $(Ni_{50}Fe_{50} + Cu)/S$ reaches a maximum value of 1.8% at a content of Cu of 68% [35]. On the other side, as Ref. [35] demonstrates, the sensitivity of the magnetoresistance of film samples to the magnetic field also depends on the component composition and reaches the maximum at 68% of Cu. It allows concluding that this concentration is optimal for GMR realization in $(Ni_{50}Fe_{50} + Cu)/S$ system. Additional investigation has shown that the value of MR effect nonmonotonically changes at the increase of mean nanoparticle size. The maximum value was obtained at L = 3.5 nm (Fig. 9, *b*). The following growth of the L value causes the fall in the magnitude of the MR effect. This is explained by the formation of a multidomain magnetic state in isolated magnetic nanoparticles [47].

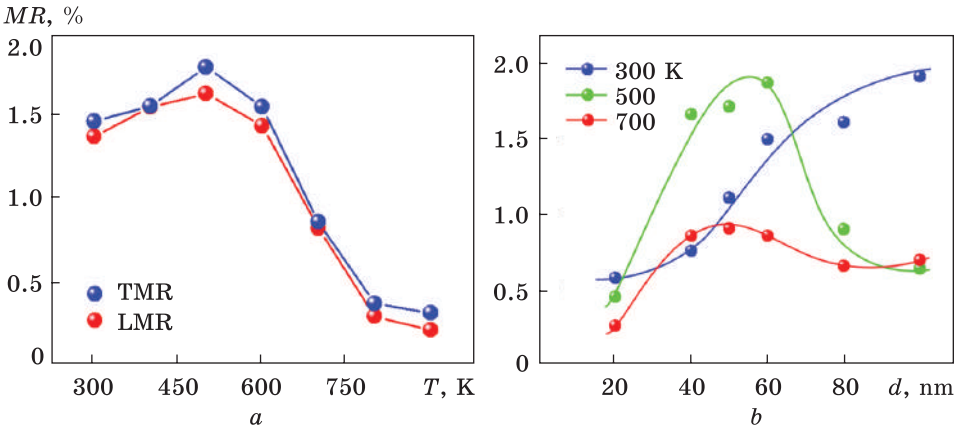

Fig. 7. Longitudinal (LMR) and transverse (TMR) magnetoresistance as a function of the annealing temperature for the annealed $(Ni_{80}Fe_{20} + Ag)/S$ film system with $d = 60$ nm and $c_{Ag} = 60$ at.% [39] (*a*) and LMR value as a function of the thickness of the $(Ni_{80}Fe_{20} + Ag)/S$ samples with $c_{Ag} = 60$ at.% [49] (*b*)

For $(Ni_{80}Fe_{20} + Ag)/S$ thin-film systems [45], the maximum value of isotropic magnetoresistance reaches 6% during the measurement at room temperature in the magnetic field $B = 8.2$ T. The reduction of measurement temperature to 77 K causes the growth of *MR* value to 13%. In this case, the optimal concentration of magnetic components is 21 vol.%.

By the shape, the field dependences of *MR* can be divided into three types: cupola-like [35] one, with a sharp maximum [36], and with a double maximum [44].

Figure 6 demonstrates that the decrease of measurement temperature leads to the growth in the *MR* value [49]. At the same time, the process of heat treatment has different effects on the shape of the *MR*–field dependences and the *MR* magnitude. For example, in the case of $(Ni_{80}Fe_{20} + Ag)/S$ system, the magnetoresistance stays negative. At this, the double maxima in *MR*(*B*) dependence at weak fields disappear in comparison with as-deposited state [44]. In the case of $(Ni_{80}Fe_{20} + Au)/S$, the magnetoresistance changes a sign and decreases by 10 times [46]. An example of the temperature dependence of *MR* value is presented in Fig. 7, *a*.

The investigation of the size effect on magnetoresistive properties of nanostructured thin-film systems $(Ni_{80}Fe_{20} + Ag)/S$ within the thickness range of 20–100 nm was done in Ref. [49]. The size dependence of *MR* value is presented in Fig. 7, *b*. It can be seen that the maximum *MR* value of 1.8% is achieved at $d = 100$ nm for as-deposited samples. For samples with $d \leq 60$ nm, the heat-treatment process at 500 K leads to an increase in *MR* value from 1.45 to 1.82%. It is a result of the improvement of crystal structure and reduction of the parasitic scattering.

At the same time, for the samples with $d > 60$ nm annealed at 500 K, the value of MR decreases and reaches a minimum of about 0.6% at $d = 100$ nm. It is a result of change in the magnetic configuration of the system due formation of multidomain nanoparticles. Upon high-temperature annealing at 700 K, the magnitude of MR fall because of increasing the probability of the electron–phonon scattering that prevents the transition of charge carriers from one ferromagnetic particle to another one. Besides, the transition to anisotropic magnetoresistance is observed.

4. Conclusions

For systems based on Ni_xFe_{1-x} permalloys and noble metals, the two-phase state is observed in an as-deposited state regardless of the preparation method. Upon annealing, the formation of solid solutions is possible.

The crystal structure of the samples is nanodimensional in as-deposited and annealed states. The mean size of ferromagnetic nanoparticles in as-deposited state does not exceed 6 nm. High-temperature annealing at a temperature of 900 K causes their growth to 20 nm.

The GMR effect was observed for the systems prepared by the layer-by-layer and co-evaporation methods. The mean reason is the realization of different mechanisms of spin-dependent electron scattering. The value of the magnetoresistive effect depends on the thickness of magnetic and nonmagnetic layers for samples prepared by the method of layer-by-layer condensation (Ni_xFe_{1-x}/NM/Ni_xFe_{1-x} and $[Ni_xFe_{1-x}]_n$). In the case of nanostructured thin-film systems prepared by the co-evaporation method (Ni_xFe_{1-x} + NM), the magnitude of the MR effect depends on the component concentration and total thickness of the samples.

The experimental results indicate the possibility of using the method of layer-by-layer condensation with subsequent heat treatment in a vacuum at a temperature of 500 K to obtain granular films. Such structures are characterized by the high thermostability of magnetoresistive properties.

Acknowledgment. This work was supported by the State Program of the Ministry of Education and Science of Ukraine within the project ‘Correlation between magnetoresistive and magnetic properties and electronic structure of multicomponent alloy films’ (State Reg. No. 0120U102005).

REFERENCES

1. M. Volmer and J. Neamtu, *J. Magn. Magn. Mater.*, **322**: 1631 (2010); https://doi.org/10.1016/j.jmmm.2009.06.085
2. Q.H. Tran, O. Sunjong, J. Jong-Ryul, and K. CheolGi, *Sens. Actuat. A*, **157**: 42 (2010); https://doi.org/10.1016/j.sna.2009.11.033
3. B.V. Neamtu, I. Chicinas, O. Isnrd, F. Popa and V. Pop, *Intemetallics*, **19**: 19 (2011); https://doi.org/10.1016/j.intermet.2010.09.004

4. S.A. Nepijko, O.V. Pylypenko, L.V. Odnodvorets, E. Kisker, H.J. Elmers, and G. Schönhense, *Appl. Phys A*, **111**: 557 (2013); https://doi.org/10.1007/s00339-012-7257-z
5. S. Wang, T. Gao, C. Wang, and J. He, *J. Alloy Compd.*, **554**: 405 (1013); https://doi.org/10.1016/j.jallcom.2012.12.004
6. Y.-T. Chen, J.-Y. Tsen, T.-S. Shey, Y.C. Lin, and S.H. Lin, *Thin Solid Films*, **544**: 602 (2013); https://doi.org/10.1016/j.tsf.2012.12.058
7. Ia. M. Lytvynenko, I. M. Pazukha, O. V. Pylypenko, and V. V. Bibyk, *Metallofiz. Noveishie Tekhnol.*, **37**, No. 10: 1377 (2015); https://doi.org/10.15407/mfint.37.10.1377
8. A.L.R. Souza, M.R. Araujo, W. Acchar, R.D. Della Pace, A.S. Melo, F. Bohn, and M.A. Correa, *Appl. Phys. A*, **125**: 236 (2019); https://doi.org/10.1007/s00339-019-2534-8
9. L. Chen, Y. Zhou, C. Lei, and Z.-M. Zhou, *Mater. Sci. Eng. B*, **172**: 101 (2010); https://doi.org/10.1016/j.mseb.2010.04.026
10. H. Kuru, H. Kockar, and M. Alper, *J. Supercond. Nov. Magn.*, **26**: 779 (2013); https://doi.org/10.1007/s10948-012-1979-1
11. H. Kuru, H. Kockar, and M. Alper, *J. Magn. Magn. Mater.*, **444**: 132 (2017); https://doi.org/10.1016/j.jmmm.2017.08.019
12. M. Kateb, J.T. Gudmundsson, and S. Ingvarsson, *J. Magn. Magn. Mater.*, **538**: 16288 (2021); https://doi.org/10.1016/j.jmmm.2021.168288
13. H. Vigo-Cotrina and A.P. Guimarres, *J. Magn. Magn. Mater.*, **497**: 166009 (2020); https://doi.org/10.1016/j.jmmm.2019.166009
14. B. Dieny, *Spin Valves: Magnetoelectronic* (Ed. M. Johnson) (Academic Press: 2004), p. 67.
15. I.V. Cheshko, M.V. Kostenko, V.I. Hrebynakha, A.M. Lohvynov, S.I. Protsenko, *J. Nano- Electron Phys.*, **8**: 03041 (2016); https://doi.org/10.21272/jnep.8(3).03041
16. Ku Hoon Chung, Si Nyeon Kim, Sang Ho Lim, *Thin Solid Films*, **650**: 44 (2018); https://doi.org/10.1016/j.tsf.2018.01.062
17. U.D. Chacyn Hernandez, M.A. Sousa, F.J. Litterst, V.P. Nascimento, and E. Baggio-Saitovitch, *J. Magn. Magn. Mater.*, **390**: 114 (2015); https://doi.org/10.1016/j.jmmm.2015.04.094
18. K. Zhao, Y. Xing, J. Han, J. Feng, W. Shi, B. Zhang, and Z. Zeng, *J. Magn. Magn. Mater.*, **432**: 10 (2017); https://doi.org/10.1016/j.jmmm.2017.01.066
19. W. Tang, Z.-W. Zhou, X.-G. Wang, Y.-Z. Nie, Q.-L. Xia, Z.-M. Zeng, R. Xiong, and G.-H. Guo, *J. Magn. Magn. Mater.*, **482**: 274 (2019); https://doi.org/10.1016/j.jmmm.2019.03.071
20. K. Anand, C. Paul, and S. Kumar, *Solid State Commun.*, **307**: 113811 (2020); https://doi.org/10.1016/j.ssc.2019.113811
21. Z. Wang, B. Dai, Y. Ren, S. Tan, J. Ni, and Jun Li, *J. Mater. Sci. Mater.*, **30**: 18328 (2019); https://doi.org/10.1016/j.jmmm.2017.01.066
22. O.E. da Silva, J.V. de Siqueira, P.R. Kern, W.J.S. Garcia, F. Beck, J.N. Rigue, and M. Carara, *J. Magn. Magn. Mater.*, **451**: 507 (2018); https://doi.org/10.1016/j.jmmm.2017.10.043

23. K.A. O'Grady, L.E. Fernandez-Outon, and G. Vallejo-Fernandez, *J. Magn. Magn. Mater.*, **322**: 883 (2010); https://doi.org/10.1016/j.jmmm.2009.12.011
24. W. Khan, Q. Wang and X. Jin, *Materials*, **11**: 439 (2018); https://doi.org/10.3390/ma11030439
25. C. Liang, C.P. Gooneratne, Q.X. Wang, Y. Liu, Y. Gianchandani, and J. Kosel, *Biosensors*, **4**: 189 (2014); https://doi.org/10.3390/bios4030189
26. M. Guruprasad, V. Srinivas, and V.V. Rao, *J. Alloys Compd.*, **484**: 851 (2009); https://doi.org/10.1016/j.jallcom.2009.05.058
27. I.Y. Protsenko, P.K. Mehta, L.V. Odnodvorets, C.J. Panchal, K.V. Tyshchenko, Y.M. Shabelnyk, and N.I. Shumakova, *J. Nano- Electron. Phys.*, **6**: 01031 (2014); https://jnep.sumdu.edu.ua/en/component/content/full_article/1168
28. I.M. Pazukha, Y.O. Shkurdoda, A.M. Chornous, and L.V. Dekhtyaruk, *Int. J. Modern. Phys. B*, **33**, No. 12, 1950113 (2019); https://doi.org/10.1142/S0217979219501133
29. V.M. Grant, J. Kennedy, P. Murmu, S. Rubanov, and S.V. Chong, *J. Magn. Magn. Mater.*, **473**: 125 (2019); https://doi.org/10.1016/j.jmmm.2018.10.072
30. A.A. Timofeev, S.M. Ryabchenko, A.F. Lozenko, P.A. Trotsenko, O.V. Stogneĭ, A.V. Sitnikov, and S.F. Avdeev, *Low Temp. Phys.*, **33**: 974 (2007); https://doi.org/10.1063/1.2747075
31. I.M. Pazukha, V.V. Shchotkin, and Yu.O. Shkurdoda, *Prog. Phys. Met.*, **20**, No. 4: 672 (2019); https://doi.org/10.15407/ufm.20.04.672
32. C. Wang, Y. Zhang, P. Zhang, Y. Rong, and T.Y. Hsu, *J. Magn. Magn. Mater.*, **320**: 683 (2008); https://doi.org/10.1016/j.jmmm.2007.08.007
33. Yu.O. Tykhonenko-Polishchuk and A.I. Tovstolytkin, *J. Nano- Electron. Phys.*, **9**: 02028 (2017); https://doi.org/10.21272/jnep.9(2).02028
34. Y.O. Shkurdoda, *J. Nano- Electron. Phys.*, **9**: 04008 (2017); https://doi.org/10.21272/jnep.9(4).04008
35. C. Wang, X. Xiao, H. Hu, Y. Rong, and T.Y. Hsy, *Phys. B*, **392**: 72 (2007); https://doi.org/10.1016/j.physb.2006.11.001
36. Y.K. Yang, L.H. Chen, and Y.H. Chang, *J. Magn. Magn. Mater.*, **189**: 195 (1998); https://doi.org/10.1016/S0304-8853(98)00211-X
37. S. Stavroyiannis, *Mater. Sci. Eng.*, **90**: 180 (2002); https://doi.org/10.1016/S0921-5107(01)00943-6
38. C. Christides, S. Stavroyiannis, and D. Niarchos, *J. Appl. Phys.*, **80**: 4512 (1996); https://doi.org/10.1063/1.363823
39. I.M. Pazukha, D.O. Shuliarenko, O.V. Pylypenko, L.V. Odnodvorets, *J. Magn. Magn. Mater.*, **485**: 89 (2019); https://doi.org/10.1016/j.jmmm.2019.04.079
40. H. Kuru, H. Kockar, M. Alper, *J. Mater. Sci.: Mater. Electron.*, **26**: 5009 (2015); https://doi.org/10.1007/s10854-015-3014-3
41. S. Young, B. Dieny, B, Rodmacq, J. Mouchot, and M.H. Vaudaine, *J. Magn. Magn. Mater.*, **162**: 38 (1996); https://doi.org/10.1016/0304-8853(96)00071-6

42. S. Bouat, S. Auffret, and B. Rodmacq, *J. Magn. Magn. Mater.*, **165**: 338 (1997); https://doi.org/10.1016/S0304-8853(96)00547-1
43. Y.O. Shkurdoda, I.M. Pazukha, and A.M. Chornous, *Intermetallics*, **93**: 1 (2018); https://doi.org/10.1016/j.intermet.2017.10.007
44. B. Dieny, S.R. Teixiera, B. Rodmacq, C. Cowache, S. Auffret, O. Redon, and J. Pierre, *J. Magn. Magn. Mater.*, **130**: 197 (1994); https://doi.org/10.1016/0304-8853(94)90675-0
45. A. Pohorilyi, A. Kravets, and E. Shypil, *Thin Solid Films*, **423**: 218 (2003); https://doi.org/10.1016/S0040-6090(02)01056-8
46. E. Rozenberg, A.I. Shames, G. Gorodetsky, J. Pelleg, and I. Felner, *J. Magn. Magn. Mater.*, **203**: 102 (1999); https://doi.org/10.1016/S0304-8853(99)00202-4
47. C. Wang, Z. Guo, Y. Rong, and T.Y. Hsu (Xu Zuyao), *J. Magn. Magn. Mater.*, **277**: 273 (2004); https://doi.org/10.1016/j.jmmm.2003.10.033
48. C. Wang, Y. Rong, and T.Y. Hsu (Xu Zuyao), *Mater. Lett.*, **60**: 379 (2006); https://doi.org/10.1016/j.matlet.2005.08.055
49. I.M. Pazukha, D.O. Shuliarenko, O.V. Pylypenko, S.I. Vorobiov, V. Tkáč, and E. Čižmár, *Appl. Phys. A*, 127: 306 (2021); https://doi.org/10.1007/s00339-021-04465-1

Received 15.07.2022;
in final version, 13.10.2022

І.М. Пазуха, Ю.О. Шкурдода
Сумський державний університет,
вул. Римського-Корсакова, 2; 40007 Суми, Україна

КРИСТАЛІЧНА СТРУКТУРА, ФАЗОВИЙ СТАН І МАГНЕТОРЕЗИСТИВНІ ВЛАСТИВОСТІ НАНОСТРУКТУРОВАНИХ ТОНКОПЛІВКОВИХ СИСТЕМ НА ОСНОВІ ПЕРМАЛОЮ ТА ШЛЯХЕТНИХ МЕТАЛІВ

Оглянуто та проаналізовано літературні дані щодо експериментальних результатів стосовно структурно-фазового стану та магнеторезистивних властивостей наноструктурованих плівкових систем на основі пермалойових стопів Ni_xFe_{1-x} і шляхетних металів. Показано, що, незалежно від методу формування (пошарова чи одночасна конденсації), фазовий стан системи залишається двофазним. У процесі високотемпературного відпалювання можливим є формування твердих розчинів. За застосування методу пошарової конденсації величина магнеторезистивного ефекту та характер польових залежностей залежать від товщини магнетних і немагнетних шарів у вихідному стані. У випадку застосування методу одночасної конденсації визначальними параметрами є концентрації компонентів і загальна товщина системи. Проаналізовано також вплив температури на магнеторезистивні властивості наноструктурованих плівкових систем на основі пермалойових стопів і шляхетних металів.

Ключові слова: пермалой, шляхетний метал, кристалічна структура, фазовий стан, магнетоопір, концентраційний ефект, температурний ефект.